This is a non-final version of an article published in final form in Neurotoxicology. 2016 Jul;55:58-64. doi: 10.1016/j.neuro.2016.05.004. Epub 2016 May 19.PMID: 27211850

Inhibition of the neuronal NFκB pathway attenuates bortezomib-induced neuropathy in a murine model

Albert Alé[a], Jordi Bruna[a], ..., Lesley Probert[b], Xavier Navarro[a], Esther Udina[a]

[a] Institute of Neurosciences and Department of Cell Biology, Physiology and Immunology, Universitat Autònoma de Barcelona, and Centro de Investigación Biomédica en Red sobre Enfermedades Neurodegenerativas (CIBERNED), Spain.

[b] Laboratory of Molecular Genetics, Hellenic Pasteur Institute, Athens, Greece.

Corresponding author: Dr. Esther Udina, Faculty of Medicine, Universitat Autònoma de Barcelona, 08193 Bellaterra, Spain. Email: esther.udina@uab.cat. Phone: (+34) 935811348, Fax (+34) 935812986.

Abstract

Bortezomib is a proteasome inhibitor with a remarkable antitumor activity, used in the clinic as first line treatment for multiple myeloma. One hallmark of bortezomib mechanism of action in neoplastic cells is the inhibition of nuclear factor kappa B (NFκB), a transcription factor involved in cell survival and proliferation. Bortezomib-induced peripheral neuropathy is a dose-limiting toxicity that often requires adjustment of treatment and affects patient's prognosis and quality of life. Since disruption of NFκB pathway can also affect neuronal survival, we assessed the role of NFκB in bortezomib-induced neuropathy by using a transgenic mouse that selectively provides blockage of the NFκB pathway in neurons. We observed that animals with impaired NFκB activation developed significantly less severe neuropathy than wild type animals, with particular preservation of large myelinated fibers, thus suggesting that NFκB pathway plays a role in bortezomib induced neuropathy. Therefore, inhibition of NFκB can be a promising strategy for the cotreatment of cancer and neuropathy.

Introduction

In the last 10 years, proteasome inhibitors have become a good strategy to treat some malignant neoplasms. Bortezomib is the first proteasome inhibitor approved to treat multiple myeloma and cell mantle lymphoma, and is under clinical trial evaluation in other solid neoplasms (Richardson et al., 2006). The blockade of protein degradation, mediated by the ubiquitin-proteasome system, inhibits several cell signaling pathways that lead to cell cycle arrest, apoptosis and inhibition of angiogenesis. It is widely accepted that the antineoplastic effect of bortezomib is mediated by the inhibition of nuclear factor kappa B (NFκB) (Demchenko & Kuehl, 2010; Goldberg, 2012; McConkey & Zhu, 2008), although NFκB can remain active in some cell types after bortezomib administration (Hideshima et al., 2009; Li et al., 2010). In non-stressed cells, NFκB remains on the cytoplasm bound to its inhibitor IκBα. After stress or inflammatory stimuli, IκBα protein is phosphorylated at two N-terminal serine residues, and ubiquitinated and degraded by the proteasome. The degradation of IκBα allows NFκB to be translocated to the nucleus via canonical or non-canonical cascades, where it will bind to DNA sites of NFκB responsive genes (Hideshima et al., 2009) to mediate, among other responses, cell proliferation, antiapoptosis, and cytokine secretion (Karin & Greten, 2005). In fact, the NFκB pathway is considered a prototypical proinflammatory signaling pathway, closely related with proinflammatory genes including cytokines, chemokines and adhesion molecules.

In a previous study, we observed that bortezomib administration in mice induced the translocation of NFκB to the nucleus in primary sensory neurons, together with an increase of several cytokines (Alé et al., 2014). However, NFκB is described as an ambiguous transcription factor in neurons. It may mediate neuronal survival but also can lead to inflammation. Therefore, in this study we evaluated the role of NFκB in our mouse model of bortezomib-induced peripheral neuropathy (BIPN). Firstly, we studied how bortezomib modulates expression of IκBα in dorsal root ganglia (DRG). Secondly, to specifically study the role of NFκB in BIPN, we evaluated the evolution of the neuropathy in mice with a transgenic dominant negative form of IκBα, which prevents degradation of endogenous IκBα and thereby prevents NFκB translocation to the nucleus inhibiting its activity.

Material and methods

OF1, C57BJL6 and TgNFL-dnIκBα mice aged 2.5 months were used in the study. In a first experiment, 20 mice per group (control and transgenic strain) were used to assess the role played by cytokines and IκBα after bortezomib exposure on DRG neurons. Subsequently, a second experiment was performed evaluating nerve conductions, functional status and histological outcome in the same bortezomib-induced peripheral neuropathy model with the aim to validate the role of NFκB. The experimental procedures were approved by the ethics committee of the Universitat Autònoma de Barcelona, and were carried out in accordance with the European Community Council Directives.

mRNA analysis

A group of OF1 mice (n=20) treated with bortezomib at 1 mg/kg subcutaneously twice per week and a group of untreated mice (n=20) were used to analyze the mRNA expression of cytokines during the treatment. Four animals per group were sacrificed by decapitation after deep anesthesia at 1, 2, 4, 6 and 8 weeks of treatment. DRG, spinal cord and sciatic nerves were rapidly dissected, maintained in RNA-later solution (Qiagen, Barcelona, Spain) and processed for mRNA analyses. Total RNA was extracted using RNeasy Mini kit (Qiagen) including a DNase step (RNase free DNase set, Qiagen). One microgram of RNA per sample was reverse-transcribed using 10 µmol/L DTT, 200 U M-MuLV reverse transcriptase (New England BioLabs, Barcelona, Spain), 10 U RNase Out Ribonuclease Inhibitor (Invitrogen) and l µmol/L oligo (dT), 1 µmol/L of random hexamers (BioLabs, Beverly, MA, USA). The reverse transcription cycle conditions were 25ºC for 10 min, 42ºC for 1 h and 72ºC for 10 min. We analyzed the mRNA expression of the inhibitor of nuclear factor kappa B alpha (IκB-α). Glyceraldehyde 3-phosphate dehydrogenase (GAPDH) expression was used to normalize the expression levels.

Gene-specific mRNA analyses were performed by SYBR-green real-time PCR using the MyiQ5 real-time PCR detection system (BioRad Laboratories, Barcelona, Spain). We previously fixed the optimal concentration of the cDNA to be used as template for each gene analysis to obtain reliable CT (threshold cycle) values for quantification. Realtime PCR amplification reactions contained the same amount of RT product, 10 µl of 2X QuantiMix EASY SYG KIT (Biotools, Madrid, Spain), 300 nM of forward and reverse primers, and completed with nanopure water to obtain a final volume of 20 µl. The thermal cycling conditions comprised 3 min polymerase activation at 95ºC, 40 cycles of 10 s at 95ºC for denaturation and 30 s at 60ºC for annealing and extension, followed by a DNA melting curve

for the determination of amplicon specificity. All experiments were performed in duplicate. CT values were obtained and analyzed with the BioRad Software. Fold change in gene expression was estimated using the CT comparative method ($2^{-\Delta\Delta T}$) normalizing to GAPDH CT values and relative to control samples. The fold-increase expression of samples during bortezomib treatment with respect to basal samples was calculated for each transcript, and was based on real-time PCR threshold values. The mean value was obtained from three pools of each tissue per condition in each group.

DRG cultures

Coverslips placed in a 24 wells plate were coated with 10µl/ml poly-D-lysine for two hours at 37ºC, washed, dried and further coated for two hours with 1µl/ml laminin. DRG were harvested from adult female mice treated with bortezomib during 1 week and from untreated mice as control. DRG were placed in Gey's salt solution (Sigma) with 6 mg/ml glucose. After peeling the DRG from connective tissue, samples were dissociated in 10% collagenase, 10% trypsin and 10% DNAse in Hanks without Ca-Mg for 30 min at 37ºC, shaked every 10 minutes. Cells were resuspended in adult Neurobasal A medium (Gibco) supplemented with 1X B-27, 1X penicillin/streptomycin, 1mM L-glutamine and 6mg/ml glucose and plated on 24 wells plates for 24 hours.

In vitro drug treatment

Bortezomib and a NFκB inhibitor (specific inhibitor SN50, sc-3060; SantaCruz) were dissolved in PBS and added to the culture medium 24 h after plating the DRG cells from wild type animals or TgNFL-dnIκBα mice. Neurons were then cultured for 3 days with bortezomib at a concentration of 8 nM bortezomib, which induced dysfunction and massive cell loss as shown in a previous study (Alé et al., 2015). The NFκB inhibitor was added at the same time that bortezomib at a concentration of 30µl/ml (Condello et al,. 2008).

For immunocytochemistry, cultures were fixed in 4% paraformaldehyde for 20 minutes, blocked with 1.5% normal donkey antiserum (Millipore) and incubated 2 hours with antibodies anti β-tubulin-type III (1:1000, Covance), anti TNF-α (1:200, R&D Systems) or anti neurofilament heavy chain (1:1000, Millipore), followed by 1 hour in secondary antibody.

In vivo treatment with bortezomib

Bortezomib was given at a dose of 1 mg/kg subcutaneously twice per week for 8 weeks (on days 1, 4, 8, 11, 15, 18, 22, 25, 29, 32, 36, 39, 43 and 46) (Bruna et al., 2010). Mice were distributed in different groups according to the treatment:

- Group TgNFL-dnIκBα mice receiving bortezomib (n=7): TG+BTZ
- Group C57BJL6 mice reveiving bortezomib (n=7): WT+BTZ
- Group TgNFL-dnIκBα mice receiving vehicle (n=5): control TG.
- Group C57BKL6 mice receiving vehicle (n=5): control WT.

Functional evaluation

The functional state of peripheral nerves was assessed by nerve conduction, rotarod and algesimetry tests. Functional evaluations were performed at baseline, before starting treatments, and then 4 and 6 weeks after onset of treatment.

For nerve conduction studies, the animals were anesthetized. The sciatic nerve was stimulated through a pair of needle electrodes percutaneously placed at the sciatic notch (proximal site) and at the ankle (distal site). The compound muscle action potential (CMAP) was recorded from the plantar interosseus muscle with microneedle electrodes. Similarly, the sensory compound nerve action potential (SNAP) was recorded by electrodes placed at the fourth toe near the digital nerves (Navarro et al., 1994; Verdu et al., 1999; Bruna et al., 2010).

A rotarod apparatus for small rodents (LIAP) was used to assess general sensory-motor function. The ability to remain on the rotarod for 120 seconds was taken as an index of normality (Verdu et al., 1999; Bruna et al., 2010).

The plantar algesimetry technique was used to evaluate nociceptive C fibers function. Mice were placed into a plastic box with an elevated glass floor (Plantar Algesimeter, Ugo Basile) and the light of a projection lamp was focused onto the plantar surface of one hindpaw. The time to withdraw the heated paw was obtained from a time-meter coupled with infrared detectors. The value for a test was the mean of three trials separated by 10 min of resting periods (Bruna et al., 2010).

Painful mechanical sensibility was assessed by means of an electronic Von Frey algesimeter (Bioseb, Chaville, France). Mice were placed on a wire mesh platform in a plastic enclosure, and a thin probe was applied on the plantar surface of each hindpaw with increasing pressure until the animal withdrew its paw. Paw withdrawal pressure was recorded in triplicate, with 15 min interval between stimuli, for both hindpaws at each testing day. The mean of the three trials was used for calculating the mechanical pain threshold.

Histological methods

At the end of follow up, animals were deeply anaesthetized and intracardiacally perfused with paraformaldehyde (4% in PBS). A segment of the sciatic nerve at mid-thigh was removed. The samples were fixed in glutaraldehyde-paraformaldehyde (3%-3%), washed in cacodylate buffer, post-fixed with 2% osmium tetroxide, dehydrated in graded concentrations of ethanol and embedded in epon. Light microscopy observations were performed on 0.5 μm semithin sections stained with toluidine blue. Myelinated fiber counts were made from systematically selected fields at 1000x final magnification using Image J software (NIH, Bethesda, MA). The density of myelinated nerve fibers was then derived (Gσmez et al. 1996; Bruna et al. 2010).

Plantar pads removed from perfused mice after the end of treatments were postfixed in Zamboni's fixative overnight and thereafter cryoprotected. Cryotome sections 70 μm thick were washed free-floating in PBS with 0.3% Triton-X100 and 1% normal goat serum for 1 h, then incubated in primary rabbit antiserum against protein gene product 9.5 (PGP9.5, 1:1000; Ultraclone). After washes, sections were incubated in secondary antiserum conjugated to cyanine 3 (Navarro et al., 1995). The sections were mounted on gelatin-coated slides and viewed in an epifluorescence microscope (Olympus BX51). Five sections from each sample were used to quantify the number and density of nerve fibers present in the epidermis of the paw pads.

Data analysis

Results are expressed as mean and standard error. The results of functional tests during the study period are expressed as the percentage with respect to baseline values for each mouse. Comparisons between experimental groups in functional tests were made using repeated measures ANOVA, and in histological, immunohistochemical, results by one-way ANOVA. For real-time PCR two ways ANOVA was used. Bonferroni test was used as the post hoc test when needed. A p value < 0.05 was considered significant.

Results

IκBα expression during bortezomib treatment in wild type animals

We found an increased mRNA expression of IκBα in DRG of animals treated with bortezomib (Fig. 1A). This increase was observed during all the treatment period, with a two fold increase at two weeks (2.40±0.82), a maximum peak at the fourth week (4.95±1.19) and a 2.5 fold increase at the end of follow up (2.52±0.36), being these values significantly higher than in control samples. Basal levels were recovered upon withdrawal of bortezomib administration.

Bortezomib neurotoxicity in sensory neurons of TgNFL-dnIκBα and WT mice

Dissociated sensory neurons from WT animals treated with 8nM bortezomib had no growing neurites at three days (Fig. 1B,F) whereas neurons from TgNFL-dnIκBα extended neurites with a normal appearance. However, only neurofilament positive neurons were able to extend neurites. Since the transgene was under neurofilament promoter, NFκB inhibition should be restricted to the subpopulation of neurofilament positive neurons (Fig 1C,G). To confirm this point, we cultured DRG from WT mice and exposed them to bortezomib alone or combined with a NFκB inhibitor (SN50). Both neurofilament positive and neurofilament negative neurons extended neurites in the presence of SN50 in the medium, indicating that inhibition of NFκB effectively protected the different populations of neurons (Fig. D,H). The percentage of neurons that were able to grow neurites was significantly higher in presence of the NFκB inhibitor (56±9%) compared to neurons exposed only to bortezomib (15±3%) (Fig. 1E).

Nerve conduction test results

The amplitude of the CMAP of both tibialis anterior and plantar muscles and the motor NCV were close to normal values during all the treatment period in both WT and TgNFL-dnIκBα mice (Fig. 2A). On the other hand, the amplitude of the SNAP of digital nerves in animals of the WT group suffered a significant and progressive decrease with respect to control values (Fig. 2B). At the end of follow up, the reduction was about 28%. In contrast, this reduction was only of about 7% in TgNFL-dnIκBα mice. Furthermore, and in contrast to proximal sensory NCV (Fig. 2C), distal sensory NCV (Fig. 2D) was significantly decreased at 8 week of follow-up in WT animals ($p=0.035$) while TgNFL-dnIκBα mice maintained normal values (Fig. 2D). In addition, WT and TgNFL-dnIκBα mice treated only with vehicle solution did not show significant differences compared to basal values (data not shown).

Algesimetry results

Thermal nociception evaluated by the plantar test showed a progressive increase of withdrawal thresholds in bortezomib treated mice, indicative of hypoesthesia. Basal values averaged 10.53±0.92 seconds for WT animals and 10.61±1.34 seconds for TgNFL-dnIκBα mice. Eight weeks after treatment the withdrawal latency increased in WT mice (12.66±1.01 s), whereas TgNFL-dnIκBα mice maintained normal latencies (10.8±1.08 s). However, these differences were not significant (Fig. 3A).

Mechanical nociception evaluated by Von Frey test showed a progressive increase of the withdrawal threshold, with a pattern similar to that observed for thermal algesimetry in animals treated with bortezomib, thus indicating reduced mechanical sensibility (5.77±0.40 gr at the end of the treatment). Although TgNFL-dnIκBα mice showed a less progressive increase in the withdrawal thresholds, (5.53±0.54 at the end of the treatment) this trend was not significant (Fig. 3B).

Histopathological results

The sciatic nerves of bortezomib-treated mice showed a well-preserved architecture. Some signs of Wallerian degeneration were observed, but without marked infiltration of macrophages. Nerves from treated animals showed a lower density of myelinated fibers in some regions of the transverse sections compared to control nerves (Fig. 4A). WT treated animals had a significant 20% reduction in the estimated number of myelinated fibers (3476 ± 251) in the sciatic nerve compared to WT control values (4250 ± 334), while TgNFL-dnIκBα treated mice showed a non significant decrease (only 6%) in the number of axons (3546 ± 382) compared with their respective controls (3761 ± 28).

Skin innervation

The number of free nerve endings in the epidermis of plantar pads, labeled with the pan neuronal marker PGP9.5, was similar between groups at the end of bortezomib treatment (19±1.1 fibers for WT and 20±2 fibers for TgNFL-dnIκBα mice), showing a significant decrease in the total number of intraepidermical fibers compared to the respective control vehicle administered groups (29±1.5 fibers and 27±2 fibers for WT and TgNFL-dnIκBα mice respectively) (Fig. 4B).

Discussion

In this study we evaluated the involvement of NFκB signaling in the induction of peripheral neuropathy by the proteasome inhibitor bortezomib. Our results show that the pharmacological blockade of cannonical NFκB activation in DRG neurons rescues the extension of neurites that is inhibited by bortezomib, and that transgenic mice overexpressing a dominant negative form of IκBα, that prevents inducible NFκB activation, suffer a less severe neuropathy that wild type animals. Together, these results indicate that NFκB plays a key role in the peripheral neurotoxicity induced by bortezomib.

Primary sensory neurons of the DRG are the first target affected by BIPN (Alé et al., 2014; Alé et al., 2015; Bruna et al., 2010). In a previous study, we evaluated the role of NFkB pathway in the neurotoxicity induced by bortezomib in DRG neurons (Alé et al., 2014). Since IκBα is degraded by the proteasome and, thus, there is an increase of IκBα with bortezomib administration, it was assumed that bortezomib was blocking NFκB activation. However, in DRG of animals treated for one week with bortezomib, we observed activation of the NFκB pathway, in coincidence with an early peak of TNFα mRNA expression, even if levels of IκBα were increased. This increased amount of IκBα protein was not related with increased mRNA expression, suggesting that there is an accumulation of IκBα in the cytoplasm due to proteasome inhibition. Therefore, , NFκB activation in this model is independent of IκBα degradation. thus further studies are needed to evaluate by which mechanism bortezomib induces NFκB activation. On the other hand, the role of NFκB in neurodegeneration is controversial, due to its double pro-apoptotic and anti-inflammatory roles (Mincheva-Tasheva & Soler, 2013). In this sense, it can be hypothetized that acute activation of the NFκB pathway leads to neuroprotection, whereas chronic activation facilitates neurodegeneration.

In order to further understand the role of NFκB pathway in the neurotoxicity induced by bortezomib, we took advantage of the TgNFL-dnIκBα mice. Addition of bortezomib to the culture medium compromised survival and markedly reduced the ability of DRG sensory neurons to extend neurites after 3 days in culture, as previously reported (Alé et al. 2015). In contrast, neurons from transgenic TgNFL-dnIκBα mice were able to extend neurites similarly to non treated neurons. Moreover, addition of a NFκB inhibitor to the culture of WT DRG neurons had a similar effect. Disruption of cytoskeleton proteins by bortezomib has been already described *in vitro* (Meregalli et al., 2013; Staff et al., 2013; Alé et al., 2015). Interestingly, Rossette and Karin (1995) showed that depolymerization of microtubules can induce NFκB nuclearization and activation, thus promoting inflammatory gene expression.

By using an *in vivo* model, we have corroborated our *in vitro* findings that NFκB is an important player in the development of BIPN. The evolution of the neuropathy in C57BJL6 WT animals was similar to the one described previously in our lab using OF1 mice (Bruna et al., 2010). In both strains, the administration regime used induced a predominantly sensory neuropathy, similar to the neuropathy observed in treated patients, as evidenced by a progressive decrease of SNAP amplitude, with no alteration of CMAP. In contrast, TgNFL-dnIκBαα mice developed significantly milder neuropathy, with a non significant decrease in the amplitude of the SNAP, and preservation of the number of myelinated fibers of the sciatic nerves of transgenic animals compared to controls. In contrast, when analyzing small nerve fiber results, the increase of withdrawal thresholds was only slightly less pronounced in TgNFL-dnIκBα mice compared to WT mice, and the loss of unmyelinated intraepidermal fibers was similar in both treated groups. It is important to take into account that nociceptive fibers are thinly myelinated or unmyelinated and, therefore, have lower amounts of neurofilament protein than myelinated axons of higher caliber (Hsieh et al., 1994). Since in transgenic animals the mutated gene is under neurofilament promoter, neurons that are neurofilament positive (myelinated ones) present more marked inhibition of the NFκB pathway. In fact, in our in vitro experiments, only the subpopulation of neurofilament positive transgenic neurons was able to extend neurites when exposed to bortezomib. In contrast, this selective effect was not found when using an inhibitor of NFκB in cultures treated with bortezomib, thus suggesting that NFκB pathway is relevant in the neurotoxicity induced by bortezomib in all types of sensory neurons. Moreover, NFκB can also affect genes related with pain, such as CGRP (Bowen et al., 2006), and thus, its inhibition could interfere with normal nociceptive function, masking a potential neuroprotection of nociceptive axons.

In summary, our results suggest that specific inhibition of NFκB may be a promising novel treatment for ameliorating BIPN. Interestingly, bortezomib induces inhibition of NFκB in multiple myeloma cells, whereas its activation in neurons is related with its toxic effects. Therefore, inhibiting NFκB could both exert a synergistic action, potentiating the antineoplastic role of bortezomib and protecting sensory neurons from its neurotoxicity.

Acknowledgments

This work was supported by Action COST-B30 of the EC, CIBERNED and TERCEL funds from the Fondo de Investigación Sanitaria of Spain. Janssen Research and Development, and Millennium Pharmaceuticals, Inc., Cambridge, MA, USA, provided bortezomib The authors

are grateful to the technical help of Mónica Espejo, Jessica Jaramillo and Marta Morell. We thank Edward M. Schwartz for the dnIκB plasmid.

Figure legends

Fig 1. Expression of IκBα mRNA in DRG from wild type mice treated with bortezomib for 1, 2, 4, 6 or 8 weeks. There was an increase in the expression of IκBα during the treatment (A). Dissociated sensory neurons culture exposed to 8 nM bortezomib for 3 days *in vitro*. Control neurons receiving bortezomib showed reduced number of neurons with neurites (black bar) compared to neurons receiving bortezomib plus an NFκB inhibitor (white bar) (E). Most neurons of WT animals lost their neurites after bortezomib treatment (B). Neurons of TgNFL-dnIκBα mice that were neurofilament positive showed growing neurites in presence of bortezomib (C), whereas non-neurofilament neurons had no neurites, similar to WT animals (G). Addition of NFκB inhibitor in the medium prevented the loss of neurites in both neurofilament positive (D) and negative neurons (H) of WT animals. Images taken at 20x. Scale bar= 25µm. Values expressed as mean±SEM. *p<0.05, **P<0.01.

Fig 2. Mean amplitude of CMAPs of plantar muscles (A) and SNAPs of digital nerves (B), proximal (from ankle to toe, C) and distal (from sciatic notch to ankle, D) sensory NCV in WT and TgNFL-dnIκBα mice treated during 8 weeks with bortezomib. Values expressed as percentages with respect to baseline. Values expressed as mean±SEM. *p<0.05.

Fig 3. Thermal algesimetry test results, expressed as time to withdrawal to hot pain stimulation (A). Mechanical algesimetry test results, expressed as withdrawal threshold to mechanical stimulation by Von Frey device (B). Groups of WT and TgNFL-dnIκBα mice were treated with bortezomib during 8 weeks. Values in TgNFL-dnIκBα animals were closer to baseline, but not significantly better than the ones obtained in WT animals. Values are expressed as percentages with respect to baseline. Values expressed as mean±SEM. *p<0.05.

Fig 4. Histogram showing the number of myelinated fibers counted in the sciatic nerve (A), and the number of intra-epidermal nerve profiles in the plantar skin (B). Wild type animals treated with bortezomib (BTZ) after 8 weeks had less myelinated fibers compared with their controls, whereas TgNFL-dnIκBα mice treated with bortezomib had a number of myelinated fibers similar to their controls (A). The number of unmyelinated fibers labeled with PGP 9.5 in the skin of treated mice showed similar reduction in both wild type and TgNFL-dnIκBα mice (B). Values expressed as mean±SEM. *p<0.05.

References

Alé, A., Bruna, J., Herrando, M., Navarro, X., & Udina, E. (2015). Toxic effects of bortezomib on primary sensory neurons and Schwann cells of adult mice. Neurotoxicity Research, 27, 430-440.

Alé, A., Bruna, J., Morell, M., van de Velde, H., Monbaliu, J., Navarro, X., & Udina, E. (2014). Treatment with anti-TNF alpha protects against the neuropathy induced by the proteasome inhibitor bortezomib in a mouse model. Experimental Neurology, 253, 165-173.

Beg, A., Baldwin, A.S. (1993). The I kappa B proteins: multifunctional regulators of Rel/NF-kappa B transcription factors. Genes and development, 15 7(11):2064-70.

Brown, K, Park, S, Kanno, T, Franzoso, G, & Siebenlist, U. (1993). Mutual regulation of the transcriptional activator NF-kappa B and its inhibitor, I kappa B-alpha. Proceedings of the National Academy of Sciences of the United States of America, 15(90), 2532-6.

Bruna, J., Udina, E., Alé, A., Vilches, J. J., Vynckier, A., Monbaliu, J., Silverman, L., Navarro, X. (2010). Neurophysiological, histological and immunohistochemical characterization of bortezomib-induced neuropathy in mice. Experimental Neurology, 223(2), 599–608.

Condello, S., Caccamo, D., Currò, M., Ferlazzo, N., Parisi, G., & Ientile, R. (2008). Transglutaminase 2 and NF- κ B interplay during NGF-induced differentiation of neuroblastoma cells. Brain Research, 1207, 1-8.

Demchenko, Y. N., & Kuehl, W. M. (2010). A critical role for the NF-κB pathway in multiple myeloma. Oncotarget, 1, 59–68.

Drive, T. C., & Francisco, S. S. (1997). Transcription factor NF-κB is activated in primary neurons by amyloid beta peptides and in neurons surrounding early plaques. Proceedings of the National Academy of Sciences of the United States of America, 94, 2642–2647.

Goldberg, A. L. (2012). Development of proteasome inhibitors as research tools and cancer drugs. The Journal of Cell Biology, 199(4), 583–8.

Hideshima T., Ikeda H., Chauhan D., Okawa Y., Raje N., Podar K., Mitsiades C., Munshi N.C, Richardson P.G, Carrasco R.D, & Anderson K.C..(2009). Bortezomib induces canonical nuclear factor-kappaB activation in multiple myeloma cells. Blood, 114(5), 1046–52.

Hunot S., Brugg B., Ricard D., Michel P., Muriel M.P. , Ruberg M. , Faucheux B.A., Agid Y., & C. Hirsch E.C.(1997). Nuclear translocation of NF-κB is increased in dopaminergic

neurons of patients with Parkinson disease. Proceedings of the National Academy of Sciences of the United States of America, 94, 7531–7536.

Hsieh, S., Kidd, G.J, Crawford, T.O, Xu, Z., Lin, W.M., Trapp, B., Cleveland, D., & Griffin, J. (1994). Regional modulation of neurofilament organization by myelination in normal axons. Journal of Neuroscience, 14(11), 6392-401.

Karin, M., & Greten, F. R. (2005). NF-κB: linking inflammation and immunity to cancer development and progression. Nat Rev Immunol, 5(10), 749–759.

Li, C., Chen, S., Yue, P., Deng, X., Lonial, S., Khuri, F. R., & Sun, S.-Y. (2010). Proteasome inhibitor PS-341 (bortezomib) induces calpain-dependent IkappaB(alpha) degradation. The Journal of Biological Chemistry, 285(21), 16096–104.

McConkey, D. J., & Zhu, K. (2008). Mechanisms of proteasome inhibitor action and resistance in cancer. Drug Resistance Updates

: Reviews and Commentaries in Antimicrobial and Anticancer Chemotherapy, 11(4-5), 164–79.

Meregalli C, Chiorazzi A, Carozzi VA, Canta A, Sala B, Colombo M, Oggioni N, Ceresa C, Foudah D, La Russa F, Miloso M, Nicolini G, Marmiroli P, Bennett DL, & Cavaletti G. (2013). Evaluation of tubulin polymerization and chronic inhibition of proteasome as citotoxicity mechanisms in bortezomib-induced peripheral neuropathy. Cell Cycle, 13(4), 1–10.

Mincheva-Tasheva, S., & Soler, R. M. (2013). NF-κB signaling pathways: role in nervous system physiology and pathology. The Neuroscientist, 19(2), 175–94.

Richardson, P. G., Briemberg, H., Jagannath, S., Wen, P. Y., Barlogie, B., Berenson, J., Singhal S, Siegel DS, Irwin D, Schuster M, Srkalovic G, Alexanian R, Rajkumar SV, Limentani S, Alsina M, Orlowski RZ, Najarian K, Esseltine D, Anderson KC,& Amato, A.. (2006). Frequency, characteristics, and reversibility of peripheral neuropathy during treatment of advanced multiple myeloma with bortezomib. Journal of Clinical Oncology, 24(19), 3113–20. doi:10.1200/JCO.2005.04.7779

Rosette, C., & Karin, M. (1995). Cytoskeletal control of gene expression: depolymerization of microtubules activates NF-κB. The Journal of Cell Biology, 128(6), 1111–9.

Staff, N. P., Podratz, J. L., Grassner, L., Bader, M., Paz, J., Knight, A. M., Loprinzi C.L, Trushina E,& Windebank, A. J. (2013). Bortezomib alters microtubule polymerization and axonal transport in rat dorsal root ganglion neurons. Neurotoxicology, 39C, 124–131.

Sun, S. C., Ganchi, P. A., Ballard, D. W., & Greene, W. C. (1993). NF-kappa B controls expression of inhibitor I kappa B alpha: evidence for an inducible autoregulatory pathway. Science, 259, 1912–1915.

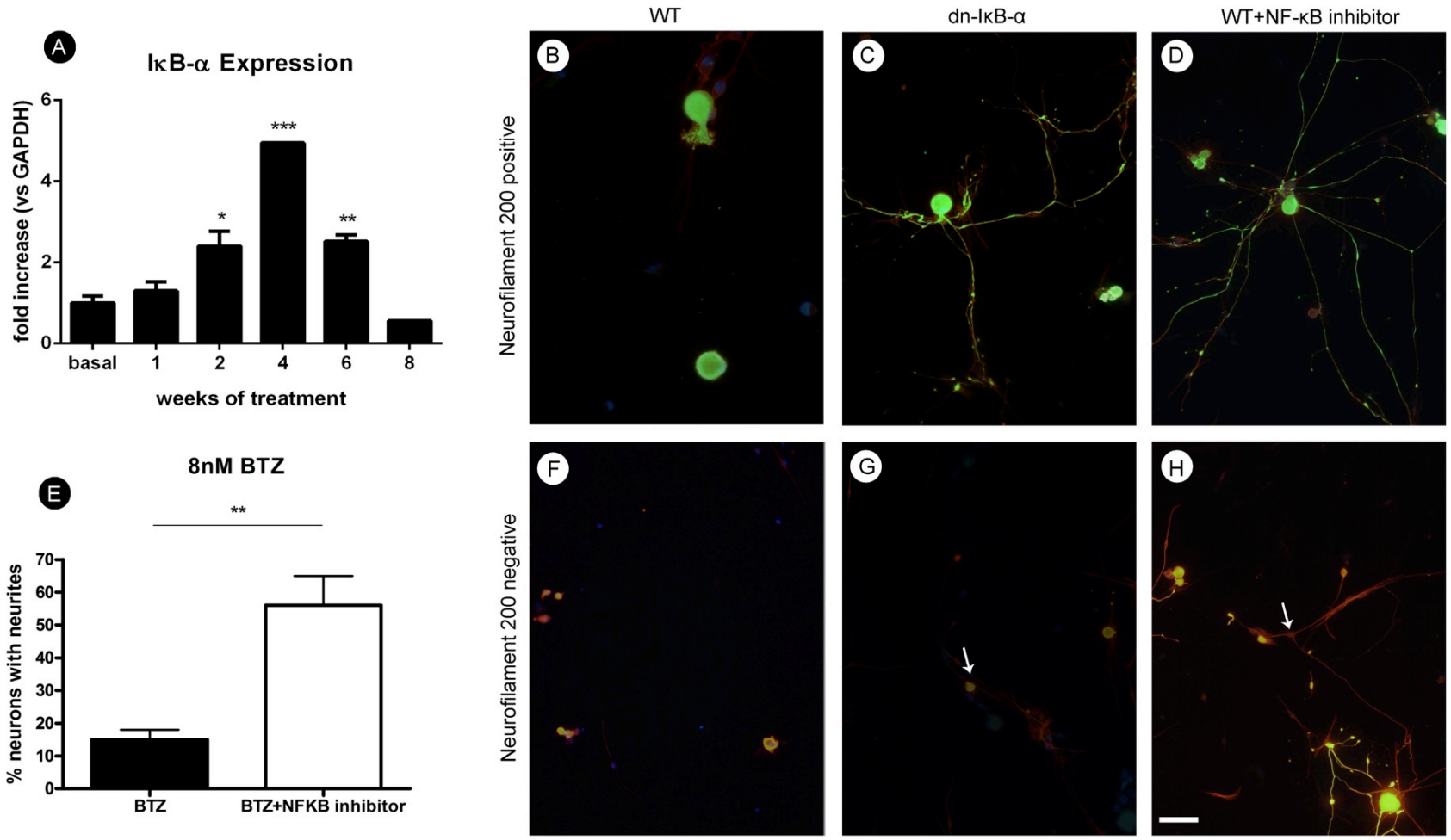

Fig 1. Expression of IκBα mRNA in DRG from wild type mice treated with bortezomib for 1, 2, 4, 6 or 8 weeks. There was an increase in the expression of IκBα during the treatment (A). Dissociated sensory neurons culture exposed to 8 nM bortezomib for 3 days *in vitro*. Control neurons receiving bortezomib showed reduced number of neurons with neurites (black bar) compared to neurons receiving bortezomib plus an NFkB inhibitor (white bar) (E). Most neurons of WT animals lost their neurites after bortezomib treatment (B). Neurons of TgNFL-dnIκB**a** mice that were neurofilament positive showed growing neurites in presence of bortezomib (C), whereas non-neurofilament neurons had no neurites, similar to WT animals (G). Addition of NFkB inhibitor in the medium prevented the loss of neurites in both neurofilament positive (D) and negative neurons (H) of WT animals. Images taken at 20x. Scale bar= 25µm. Values expressed as mean±SEM. *p<0.05, **P<0.01.

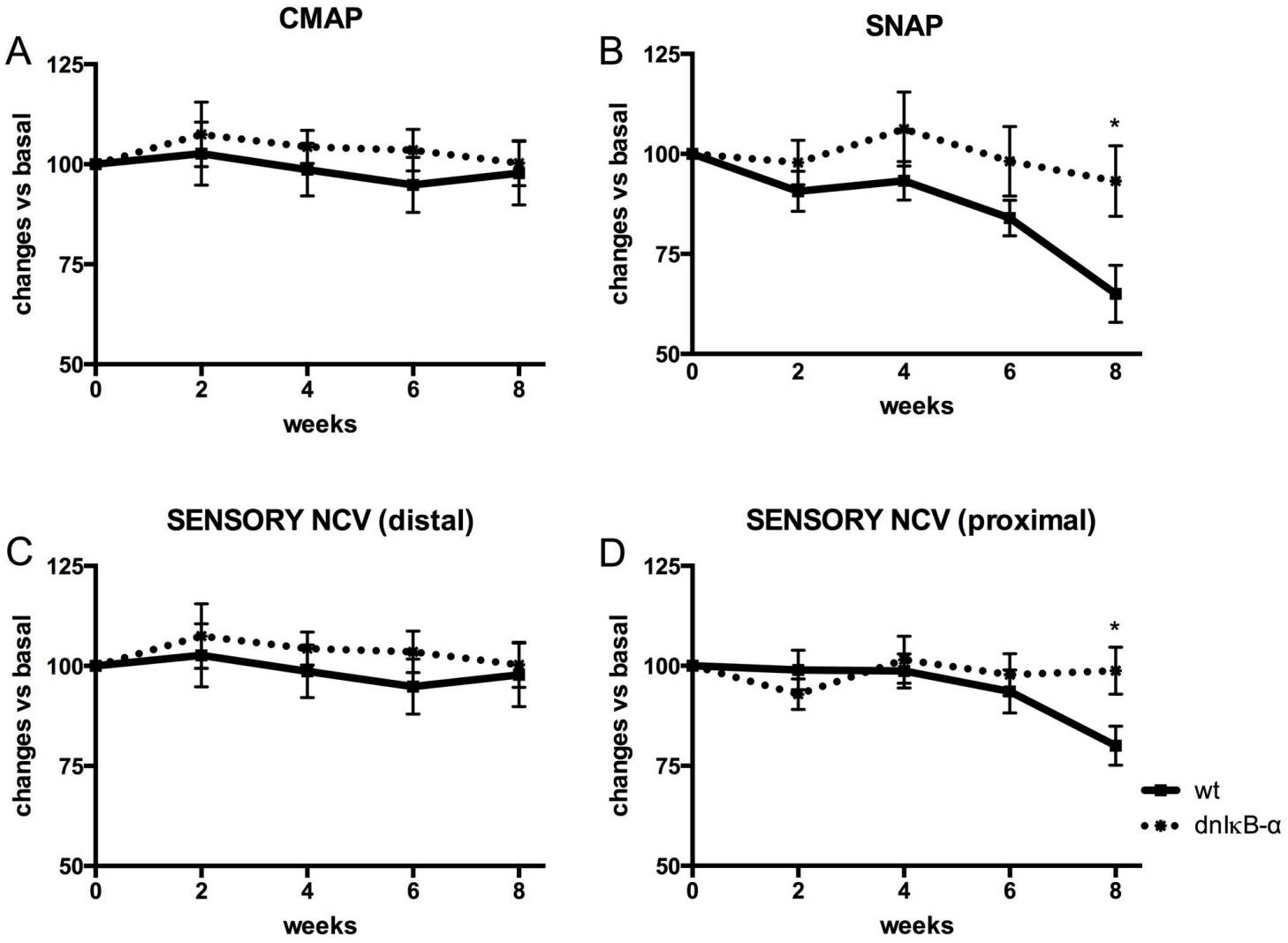

Figure. 2. Mean amplitude of CMAPs of plantar muscles (A) and SNAPs of digital nerves (B), proximal (from ankle to toe, C) and distal (from sciatic notch to ankle, D) sensory NCV in WT and TgNFL-dnIκB**a** mice treated during 8 weeks with bortezomib. Values expressed as percentages with respect to baseline. Values expressed as mean±SEM. *$p<0.05$.

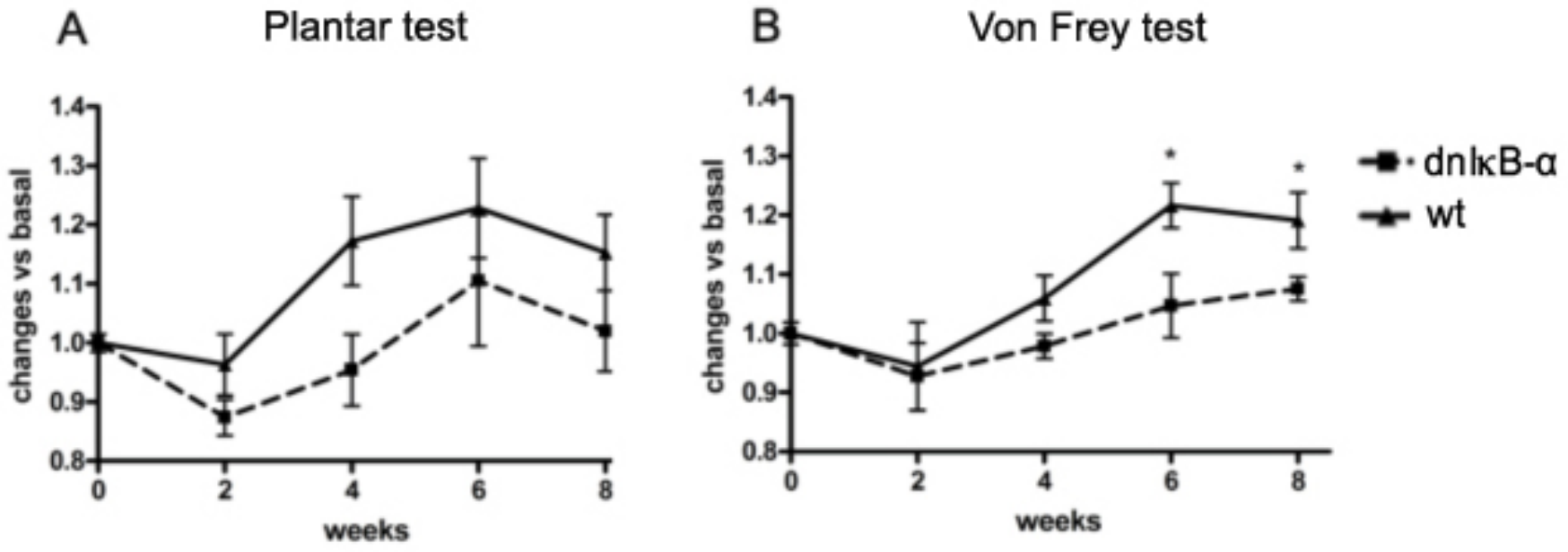

Figure 3. (A) Thermal algesimetry test results, expressed as time to withdrawal to hot pain stimulation (A). Mechanical algesimetry test results, expressed as withdrawal threshold to mechanical stimulation by Von Frey device (B). Groups of WT and TgNFL-dnIκB**a** mice were treated with bortezomib during 8 weeks. Values in TgNFL-dnIκB**a** animals were closer to baseline, but not significantly better than the ones obtained in WT animals. Values are expressed as percentages with respect to baseline. Values expressed as mean±SEM. *$p<0.05$.

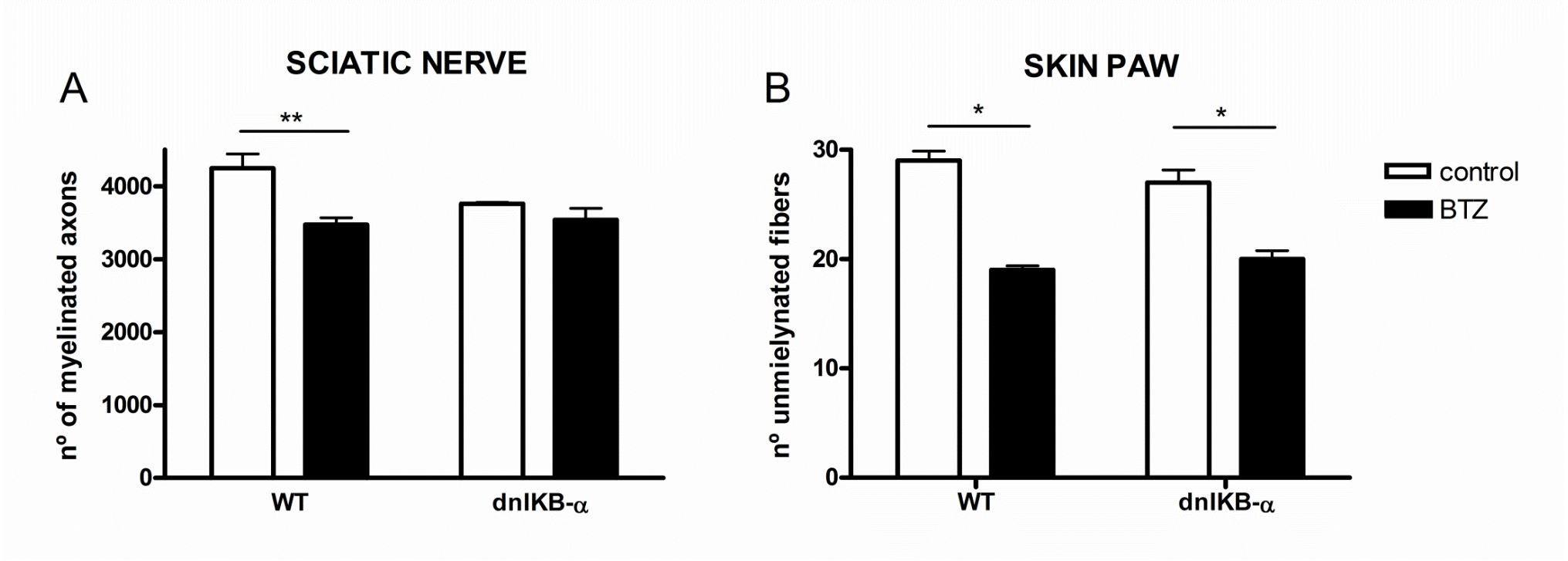

Figure 4. Histogram showing the number of myelinated fibers counted in the sciatic nerve (A), and the number of intra-epidermal nerve profiles in the plantar skin (B). Wild type animals treated with bortezomib (BTZ) after 8 weeks had less myelinated fibers compared with their controls, whereas TgNFL-dnIκB**a** mice treated with bortezomib had a number of myelinated fibers similar to their controls (A). The number of unmyelinated fibers labeled with PGP 9.5 in the skin of treated mice showed similar reduction in both wild type and TgNFL-dnIκB**a** mice (B). Values expressed as mean±SEM. *$p<0.05$.